Original Research

Genotoxic effects of photodynamic therapy in laryngeal cancer cells – An *in vitro* study

Carlos Dailton Guedes de Oliveira Moraes[1], Bruno Henrique Godoi[1], Isabel Chaves Silva Carvalho[1], Jessica Cristina Pinto[1], Rafaella Carvalho Rossato[1], Newton Soares da Silva[2] and Cristina Pacheco Soares[1]

[1]Institute of Research and Development – IP&D, Universidade do Vale do Paraíba – UNIVAP, Laboratory Dynamics of Cellular Compartments, Sao Paulo 12244-000, Brazil; [2]Institute of Research and Development – IP&D, Universidade do Vale do Paraíba – UNIVAP, Laboratory of Cell Biology and Tissue, Sao Paulo, CEP 12244-000, Brazil
Corresponding author: Cristina Pacheco Soares. Email: cpsoares@univap.br

Impact statement

Recently, the use of photodynamic therapy grows as an alternative treatment for cancer, since it has a noninvasive characteristic and affinity to the tumor tissue. Accordingly, understanding the therapy's foci of action is important for the technique improvement. This work aims to understand the genotoxic effect triggered by the therapy action, thus evidencing the permanent changes caused to the genetic material of the tumor cell after the treatment. Therefore, to increase the knowledge in this study field, the methodology of the comet assay and count of micronucleus formed after the therapy was adopted in order to understand if the damage caused to the DNA of tumor cell makes its replication process unfeasible in future generations. The study allows a better therapeutic approach to the cancer treatment, making the process of association between therapies a more effective option during the disease treatment.

Abstract

Photodynamic therapy provides the formation of reactive oxygen species that are capable of inducing cell death. Human laryngeal carcinoma (HEp-2) cells have been evaluated in this study under PDT treatment. Cells were treated with photosensitizer aluminum phthalocyanine tetrasulfonate ($AlPcS_4$) and irradiated with a Biopdi/Irrad-Led5 660 LED with 660 nm wavelength, intensity of delivered light of 25 mW/cm^2, power of 70 mW, fluence of 5 J/cm^2 for 24 h and 48 h, and then evaluated. Cell population was not increased by PDT treatment after the tested period. The apoptosis assay demonstrated that control groups exhibit approximately 60% of living cells in the 24 h and 48 h periods, however. A significant increase in apoptotic cells was observed after the photodynamic therapy treatments, for both 24 and 48 h groups. Over 50% of cells were under apoptosis after photodynamic therapy, evidencing a death process generated from the oxidative damage of the treatment. Comet assay and micronucleus assessments, both of which evaluate genotoxicity, demonstrated favorable results to damages caused by the photodynamic therapy treatment. Thus, photodynamic therapy is proposed to damage nuclear cells and the subcellular structure of carcinogenic cells.

Keywords: Cancer, photodynamic, genotoxicity, DNA, cell, damage

***Experimental Biology and Medicine* 2019; 244: 262–271. DOI: 10.1177/1535370219826544**

Introduction

Photodynamic therapy (PDT) is a treatment method that employs a photosensitive dye and suitable wavelength light in the presence of molecular oxygen. Each isolated PDT component is harmless to cells, but their interaction results in cytotoxic damage to tumor cells due to the formation of reactive oxygen species (ROS). As a result, tumor cells submitted to PDT suffer irreversible photodamage to vital target subcellular structures, including the plasma, the cell membrane, mitochondria, lysosomes, Golgi apparatuses, and endoplasmic reticulum. The damage to cancer cells and their vital subcellular structures resulting from the action of ROS can lead to cell death by either apoptosis or necrosis.[1–5]

In addition, the use of PDT in the treatment of cancer is very attractive because of its intrinsic double selectivity, i.e. the photosensitizer has a great tendency to accumulate in the malignant tissue and the irradiated light is spatially

focused onto the lesion. Another advantage of PDT is that it does not present cumulative toxicity to the patient and no maximum cumulative dose is known, as it occurs in other already established treatments such as chemo- and radiation therapy.[6,7]

Photochemical reactions occur in the cell and its compartments, since photosensitizing tends to focus on other cellular structures, such as mitochondria, endoplasmic reticulum, and lysosomes. Although DNA damage has not been decisively confirmed, some studies have clarified the interaction between PDT and DNA damage in cells.[8,9] This becomes important as DNA is the most vulnerable material in a cell and cannot be simply replaced. Damage to the cell genetic material can happen due to spontaneous basic hydrolysis as a result of natural stress or external influences.[10–12]

Currently, several photosensitizers, classified either as first, second or third generation photosensitizers, are used in PDT studies. Among them, methylene blue seems to have DNA as its main target. Since the main characteristic of methylene blue is having a cation, which can intercalate with the DNA structure, especially in regions rich in guanine-cytosine, due to its positive charge and planar geometry, it can lead to a break and oxidative degradation of the bases via singlet oxygen, thus causing DNA damage.[13–16]

It must also be considered that ROS can cause damage to macromolecules, such as lipids, as well as to proteins and even DNA, thus furthering the redox imbalance in the cell signaling pathways. As a result, the interaction between monochromatic light and the photosensitizer induces a series of photophysical and photochemical processes that produces ROS in large numbers at the end of type-I and -II reactions. A sequence of cytotoxic oxidative events then occurs in cell organelles (mitochondria, lysosomes, the cell membranes and nucleus), where ROS interacts with almost any molecule, leading to chemical modifications that impede the normal functioning of the cell through damage to the cell membrane, DNA, and other structures. Furthermore, an important biological consequence of the oxidation of proteins is the subsequent oxidation of DNA by the peroxides formed. Thus, the initial generation of peroxides and their interaction with nuclear proteins, such as histones, can also promote subsequent DNA damage.[5–7,12,17–19]

Therefore, the purpose of the present study was to evaluate the effect of PDT using aluminum phthalocyanine tetrasulfonate, a second generation photosensitizer, in cancer cell line HEp-2, for better understanding the damage caused by ROS to cell DNA. Special attention was paid to cytotoxicity, especially genotoxicity, 24 h and 48 h after the PDT treatment.

Materials and methods

Cell culture

HEp-2 (human laryngeal carcinoma ATCC – CCL – 23) cells were obtained from the Paul Ehrlich Technical Scientific Association Cell Bank (Associação Técnico Científica Paul Ehrlich - Banco de Células do Rio de Janeiro UFRJ – RJ) and cultured in 25 cm^2 bottles at 37°C under 5% CO^2 in DMEM (Dulbecco's modified Eagles medium – Thermo Fisher Scientific, Gibco, Waltham, Massachusetts, EUA) supplemented with 10% fetal bovine serum (Thermo Fisher Scientific, Gibco, Waltham, MA, EUA) and 1% penicillin and streptomycin (Thermo Fisher Scientific, Invitrogen, Waltham, MA, EUA).

Photosensitizer

Aluminum phthalocyanine tetrasulfonate ($AlPcS_4$) (Porphyrin Frontier Scientific, Logan, UT, USA) was diluted in phosphate-buffered saline (PBS) at a concentration of 5 μM and kept in the dark at 4°C until use.[20]

PDT in cells

The culture medium was removed 24 h after plating (1×10^5 cells/mL per well) in a 24-well plates and the wells were washed twice with PBS to avoid interference with the treatment. Next, 200 μL of the 10 μM pre-prepared AlPcS4 solution was added in and the cells were incubated for 1 h at 37°C under 5% CO_2 in the dark. At the end of this period, the $AlPcS_4$ solution was removed and the cells were washed again twice with PBS to remove the excess photosensitizer; 200 μL of PBS were then added to each well for the irradiation process. The LED device, Biopdi/IRRAD-LED 660 nm (Biopdi, São Carlos, São Paulo, Brazil), used for PDT irradiation consists of 54 LEDs, each individual LED has 70 mW of power, emitting in 660 ± 5 nm, and covering an area of 150 cm^2. The power density of delivered light was 25 mW/cm^2, and the exposure time was 3 min and 20 s, totalizing the fluence of 5 J/cm^2. The power density was calculated according to the following formula: $(54 \times 70)/A = I$, and the fluence was calculated according to the following one: I (W/cm^2) × t (s) = F (J/cm^2).[21] After irradiation, PBS was discarded and 500 μL of DMEM culture medium supplemented with 10% fetal bovine serum was added to the wells. Cells were maintained at 37°C under 5% CO_2 in the dark. Thus, two groups were investigated: Control group (not submitted to PDT) and the treatment group, submitted to PDT.[22]

Viability assay

Using a protocol adapted for the viability assay, non-adhered cells were discarded from the culture plate by washing with PBS at 37°C. Adhered cells were then incubated with 100 μL of crystal violet solution for 4 min at room temperature. At the end of incubation, the plate was washed with water to remove excess dye and 200 μL of elution solution (SDS – sodium dodecyl sulfate) were added for incubation for 1 h before reading using a SpectraCount – Packard 570 nm spectrophotometer. The whole process was carried out in the dark. Data collected were statistically analyzed.[23]

Mitochondrial activity assay

Mitochondrial activity was evaluated by the colorimetric MTT [(bromide 3–4,5-dimethylthiazol-2-yl) -2,5-

difeniltetrazoliol] (Sigma) assay. After PDT, 100 μL of MTT solution (5 mg/mL) were added to the wells and incubated for 2 h at 37°C in 5% CO_2. After this period, cells were incubated with 200 μL of DMSO (dimethyl sulfoxide) for 30 min under stirring and the absorbance was measured at 570 nm (SpectraCount - Packard spectrophotometer). The whole process was carried out in the dark. Data collected were statistically analyzed.[21]

Apoptosis assay

The analysis of apoptosis and necrosis is performed by image cytometer Tali® with Apoptosis Kit, enabling the identification of apoptotic cells and discrimination of apoptotic from necrotic and live cells after the PDT treatment in 24 h and 48 h periods. The kit stains apoptotic cells with green Annexin V – Alexa Fluor® 488, necrotic cells with both red propidium iodide and green Annexin V – Alexa Fluor® 488, and does not stain live cells (Invitrogen™ Tali™ Image-based Cytometer).[24]

Comet assay

HEp-2 cells were cultured in 24-well plates with cell density of 1×10^5 for 24 h and 48 h after the PDT treatment. Briefly, the cells were detached with trypsin/0.25% EDTA (Thermo Fisher Scientific, Gibco, Waltham, Massachusetts, EUA), 200 μL/well for 3 min, centrifuged (3000 r/min/5 min), resuspended in 200 μL 0.5% low-melting point agarose (Thermo Fisher Scientific, Gibco, Waltham, Massachusetts, EUA) at 37°C and transferred to newly prepared slides with 1.5% agarose (Thermo Fisher Scientific, Gibco, Waltham, Massachusetts, EUA). The slides were immersed in a fresh cold (4°C) lysis solution (2.5 M NaCl, 100 mM Na2 EDTA, 10 mM Tris-HCl, pH 10–10.5, 1% Triton X-100 and 10% DMSO) for 1 h and next placed in an electrophoresis chamber, which was then filled with freshly prepared alkaline buffer at 4°C (300 mM NaOH and 1 mM EDTA, pH 13). Electrophoresis was performed at 300 mA and 25 V for 30 min. Next, the slides were positioned horizontally and washed three times (5 min each time) with 0.4 M TRIS –HCl, pH 7.5. Finally, 30 μL of ethidium bromide (20 μg/mL) were added to each slide. All the analysis steps were conducted away from direct light to prevent additional DNA damage. Images were acquired with an epifluorescence microscope (Leica Epifluorescence Microscope DMLB with a Leica DFC310FX model camera). Ten randomly selected fields were photographed and 100 randomly selected cells per group ($n = 3$) were analyzed. Comet images were automatically analyzed using the OpenComet analysis software and statistically analyzed. The data obtained in the comet assay were percentage DNA in the comet tail, which shows tail DNA content as a percentage of comet DNA content, and Olive Moment, which shows a product of percent DNA in the comet tail and the distance between intensity-weighted head and tail centroids. These data were chosen based on Gyori *et al.*,[25] who explained the OpenComet software. The comet assay protocol was described by Singh *et al.* and used with a minor modification described in Silva and performed by Carvalho *et al.*[26–28]

Micronucleus assay

The micronucleus assay protocol used was described by Tian *et al.* and performed by Carvalho *et al.*[26,29] HEp-2 cells were cultured in 24-well plates with a cell density of 1×10^5 and evaluated in periods of 24 h and 48 h after the PDT treatment was performed as described above. After the PDT treatment, the groups were exposed to Cytochalasin B (Thermo Fisher Scientific, Invitrogen, Waltham, MA, EUA); 24 h after the PDT treatment, the control groups, control for the formation of micronuclei, and the treatment group were exposed to 200 μL of Cytochalasin B at a concentration of 3 μg/mL to interrupt cell division and facilitate the visualization of micronuclei. Then, the cells were washed with PBS twice and fixed in 4% paraformaldehyde in phosphate buffer for 10 h at room temperature. The cells were washed again with PBS and incubated with 200 μL DAPI (4′,6-Diamino-2-Phenylindole, Sigma/Aldrich, St. Louis, MO, EUA) in 300 μM phosphate buffer for 10 min at room temperature. The micronucleus experiments were performed in triplicate. The EMS group was included in this assay as a Control group for micronucleus formation. This new group was made up of cells treated with Ethyl methanesulfonate (EMS – Thermo Fisher Scientific, Invitrogen, Waltham, MA, EUA) as a genotoxic agent at a concentration of 6 μM.[30,31] The number of cells with micronuclei was counted in a fluorescence microscope (Leica Fluorescence Microscope DMIL) coupled with a Leica camera model DFC310FX to capture images and with Leica Application Suite V3 software. Images were captured in 10 different fields of each well, totaling 30 fields per experimental group. The micronucleus frequency per 100 cells presented by the PDT, EMS, and Control groups was counted after 24 h and 48 h ($n = 8$). Analyses were conducted in double-blind test for the confirmation of the number of micronuclei in the images. The criteria used to identify micronuclei were those defined by Fenech,[32] Nersesyan *et al.*,[33] and Titenko-Holland.[34] After collection, the data were statistically analyzed.

Statistical analysis

The viability assay data distribution was normal (Kolmogorov–Smirnov test) and statistical analysis was performed using a parametric test (test *t*). The comet assay data showed non-normal distribution (Kolmogorov–Smirnov test) and statistical analysis was performed using a nonparametric test (Mann–Whitney test). The micronucleus assay data distribution was normal (Kolmogorov–Smirnov test) and statistical analysis was performed using the parametric tests (ANOVA, followed by the Tukey test).

All data were analyzed in software GraphPad Prism 6.0 (GraphPad Inc., La Jolla, CA). No statistical adjustment was applied to the samples. The viability and micronucleus assay data were expressed as means ± standard deviation and the comet assay data were expressed as minimum, maximum, and median values. Statistical significance was set at 0.05.

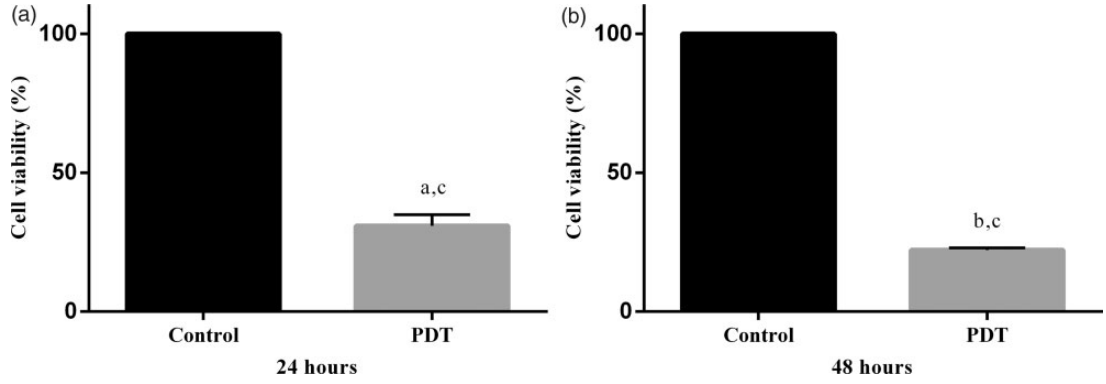

Figure 1. Cell viability verified by crystal violet assay 24 h (a) and 48 h (b) after exposure of HEp-2 Human Laryngeal Carcinoma (ATCC – CCL-23) to PDT. Cell viability, compared to the Control group, was analyzed by DNA staining with crystal violet (CV). Statistically significant differences between the PDT groups are indicated with different superscript letters ($n = 6$, test t, a and b, $P < 0.0001$, c, $P = 0.0005$).

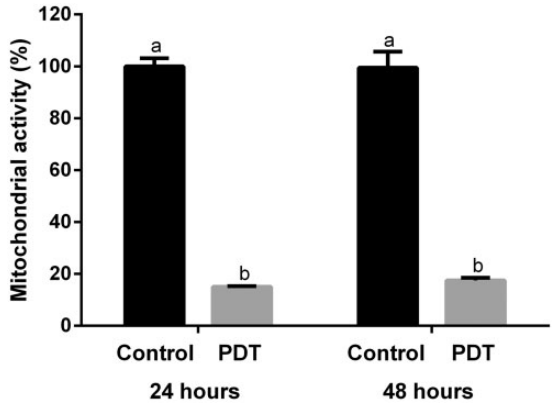

Figure 2. Mitochondrial activity was verified by MTT assay 24 h and 48 h after exposure of HEp-2 human laryngeal carcinoma (ATCC – CCL-23) to PDT. Statistically significant differences between the PDT groups are indicated with different superscript letters ($n = 6$, test t, a and b, $P < 0.0001$). In the intragroup comparison, there was no statistical difference in the control group and PDT in periods 24 h and 48 h.

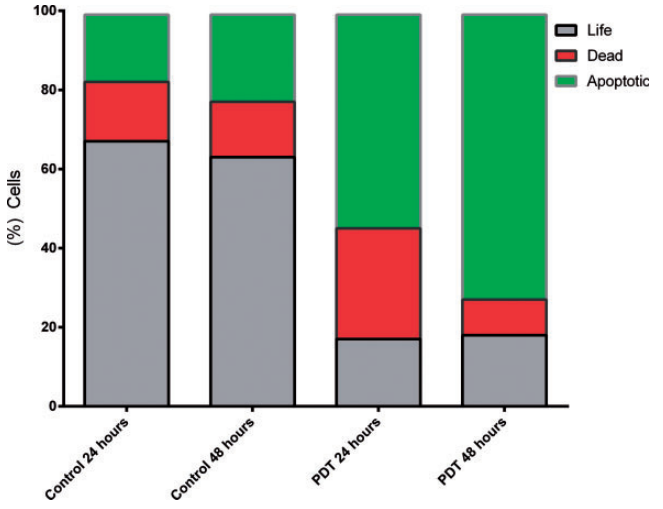

Figure 3. The type of cell death was verified through the Tali apoptosis assay kit, after exposure of HEp-2 human laryngeal carcinoma (ATCC – CCL-23) to PDT using the Tali equipment, image-base cytometer. The control group has a rate of approximately 60% of living cells, 15 to 20% of dead cells and approximately 20% of apoptotic cells in the periods of 24 h and 48 h. However, the PDT group has a rate of approximately 20% of live cells, 25% of dead cells and approximately 60% of apoptotic cells in the 24-h period. In the 48 h, the PDT group had 20% live cells, 10% dead cells and approximately 70% apoptotic cells ($n = 7$). (A color version of this figure is available in the online journal.)

Results

Viability assay

Results obtained in the colorimetric assay with violet crystal evidenced the effect of PDT on cancer cells over 24 h (Figure 1(a)) and 48 h (Figure 1(b)). The results showed statistically significant difference between the Control and the PDT groups in both periods studied ($P < 0.0001$). Additionally, the PDT group presented a statistical difference between the 24- and 48-h periods ($P = 0.0005$) (Figure 1 (a) and (b)).

Mitochondrial activity assay

According to the MTT results, the effect of PDT on cancer cells over 24 h and 48 h (Figure 2) was evidenced. The results showed statistically significant difference between the Control and the PDT groups in both periods studied ($P < 0.0001$). Additionally, Control and PDT groups did not present the statistical difference between themselves for both 24 h and 48 h periods (Figure 2).

Apoptosis assay

The results obtained with the evaluation of apoptosis using the Tali equipment, image-base cytometer, indicated that the control group had approximately 60% of living cells, 15 to 20% of dead cells, and approximately 20% of apoptotic cells in the periods of 24 h and 48 h (Figure 3). However, PDT group had a rate of approximately 20% of live cells, 25% of dead cells, and approximately 60% of apoptotic cells after 24 h. After 48 h, PDT group had also 20% live cells, 10% dead cells, and approximately 70% apoptotic cells (Figure 3).

Comet assay

PDT caused DNA damage to the cells. The percentage of DNA in the comet tail and the Olive Moment data was significantly higher in the PDT group than in the Control group ($P < 0.0001$) at 24 h (Tables 1 and 2). However, at 48 h,

the percentages of DNA in the comet tail and the Olive Moment data were not significantly different between the PDT and the Control group ($P = 0.9956$ and $P = 0.2067$, respectively) (Tables 1 and 2). Additionally, the Control group presented a statistically significant difference in the percentage of DNA in the comet tail ($P < 0.0001$) and in the Olive Moment data ($P = 0.0002$) between the 24- and 48-h periods (Figure 4).

Micronucleus assay

Various materials can cause damage to DNA, which results in formation of micronuclei, small structures close to the cell nucleus. Since EMS is a substance known to cause micronucleus formation, it is used as a standard for positive Control.

Comparison of the Control and the PDT groups and the Control and EMS groups revealed a difference between the micronucleus frequency values, both at 24 h ($P = 0.0005$ and $P < 0.0001$, respectively) and 48 h ($P < 0.0001$ and $P < 0.0001$, respectively) (Figure 5(a)). The results also showed that there was a statistical difference between the Control and the EMS groups in both periods studied (24 h, $P < 0.0001$ and 48 h, $P < 0.0001$). Furthermore, a significant increase in micronucleus frequency was observed in the Control ($P = 0.0152$) and the EMS ($P = 0.0003$) groups when the 24 h and 48 h period results were compared; however, the PDT group showed no statistic difference in these periods ($P = 0.2640$) (Figure 5(a) and (b)).

Table 1. Comet assay analysis of DNA damage in HEp-2 human laryngeal carcinoma (ATCC – CCL-23) cells submitted to PDT and Control group.

Tail DNA %	24-h Comet assay		48-h Comet assay	
Groups	Control	PDT	Control	PDT
Average	20.4[a]	64.14	45.21[a]	51.91
Median	6.282[a]	88.12	22.23[a]	49.66
Standard deviation	30.57	40.18	41.54	43.84
Minimum	0.0	0.0	1.174	1.131
25% percentile	3.093	13.98	7.976	5.773
75% percentile	15.75	98.02	97.60	97.96
Maximum	100.0	100.00	100.00	100.00
Sample size (n)[b]	300	300	300	300
P	0.0001	0.9956		

Note: DNA in the comet tail shown as a percentage of comet DNA content. The data represent the minimum, maximum, and median values of 100 randomly selected cells per group of the three independent experiments ($n = 3$ per group). Mann–Whitney test, *$P < 0.0001$, significantly different from the Control value.
[a]Statistical difference between the 24- and 48-h period Control group results ($P < 0.0001$).
(*n*)[b]Considering the number of cells analyzed in each group.
PDT: photodynamic therapy.

Table 2. Comet assay analysis of DNA damage in HEp-2 human laryngeal carcinoma (ATCC – CCL-23) cells submitted to PDT and Control group.

Olive moment	24-h Comet assay		48-h Comet assay	
Groups	Control	PDT	Control	PDT
Average	5.238[a]	12.50	10.47[a]	19.85
Median	0.8375[a]	8.978	4.335[a]	8.768
Standard deviation	25.58	19.68	15.57	33.53
Minimum	0.0	0.0	0.07042	0.0
25% percentile	0.2679	0.8044	1.011	1.006
75% percentile	2.712	17.16	13.10	25.45
Maximum	385.2	193.7	58.00	261.7
Sample size (n)[b]	300	300	300	300
P	<0.0001		0.2067	

Note: The Olive Moment shows a product of percentage of DNA in the comet tail and the distance between the intensity-weighted centroids of the head and tail. The data represent the minimum, maximum, and median values of 100 randomly selected cells per group of the three independent experiments ($n = 3$ per group). Mann–Whitney test, *$P < 0.0001$, significantly different from the Control value.
[a]Statistical difference between the 24- and 48-h period Control group results ($P = 0.0002$).
(n)[b]Considering the number of cells analyzed in each group.
PDT: photodynamic therapy.

Discussion

In the present study, cancer cells (HEp-2) were responsive to the treatment. The cell viability assay, mitochondrial activity assay, apoptosis assay, comet and micronucleus assay results demonstrated the interaction of the LED light with the photosensitizer ($AlPcS_4$) and oxygen in ROS production, which caused damage to the cancer cells.

Although PDT was very efficient in reducing cancer cells, there may be some disadvantages in its use, such as the difficulty in quantifying and localizing the photosensitizer. Moreover, the slow accumulation and heterogeneity response of the photosensitizer in the tumor tissue may influence the irradiation process, and consequently the PDT.[35,36] In addition, the period of incubation and concentration of the administered photosensitizer, without monitoring, are important parameters to be considered. Another fact to be evidenced is the late elimination and of some photosensitizer by the organism, remaining months in the skin.[37,38]

Thereby, cell viability by the violet crystal assay is performed based on a colorimetric quantitative method with the aid of a spectrophotometer, in which the colorimetric density indicates the number of cells present in the counting area;[23] therefore, analyzing the data obtained for the PDT treatment in cancer cells, it is possible to evidence the difference between the Control and PDT groups, since the PDT treatment causes direct and intense damage to cancer cells and their structures through the action of ROS, resulting in a decrease in the cell population, as confirmed by the cell viability.[39]

Moreover, it can be inferred that the PDT treatment not only decreased the cancer cell population, thus serving as a test that proves cell death, but also allowed the quantification of the viability of the cancer cells. The violet crystal test employs a basic dye that has the ability to interact with and incorporate negatively charged cellular structures, such as DNA and plasma membrane.

Thus, recent studies Xin *et al.*, Gijsens *et al.*, and Castilho-Fernandes *et al.* have demonstrated the importance of using $AlPcS_4$ photosensitizer conjugated or encapsulated in gold particles or liposomes carriers, indicating the increased

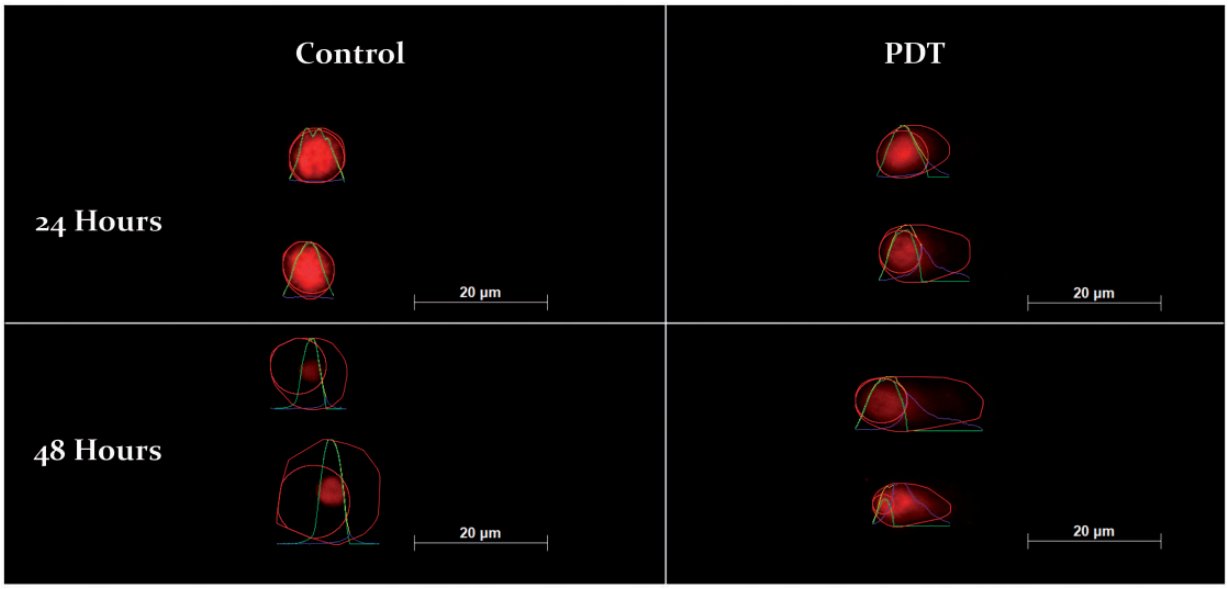

Figure 4. The formation of the comet was verified with comet assay after 24 h and 48 h exposure of HEp-2 Human laryngeal carcinoma (ATCC – CCL-23) to PDT. (A color version of this figure is available in the online journal.)

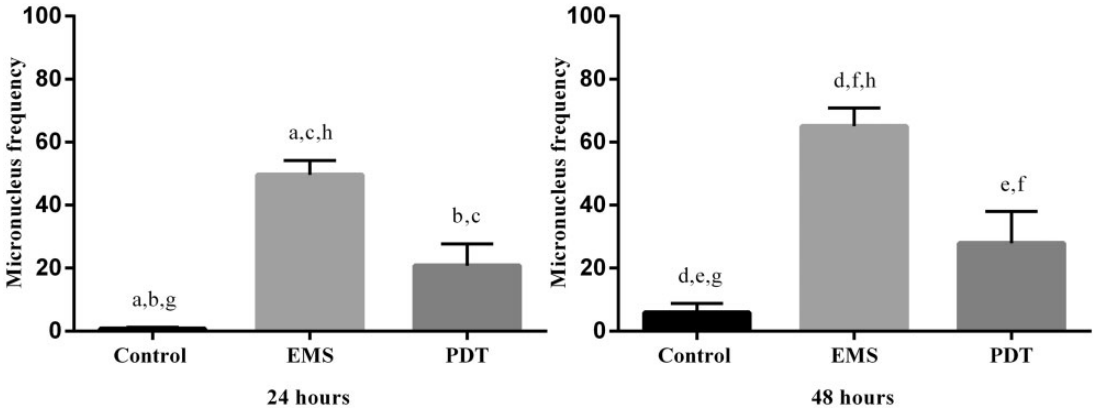

Figure 5. Micronucleus (MN) frequency in HEp-2 human laryngeal carcinoma (ATCC – CCL-23) cells PDT, EMS and Control groups per 100 cells after 24 h (a) and 48 h (b). Statistically significant difference between PDT, EMS ,and Control groups indicated with superscript letters ($n = 8$; ANOVA, Tukey Test; a, c, d, and f $P < 0.0001$; b, $P = 0.0005$; g, $P = 0.0152$; h, $P = 0.0003$).

efficiency of the photosensitizer on cell viability when compared with free administration of AlPcS4.[40–42] These applications are result of a new generation of photosensitizers, synthesized in order to increase efficiency by acting specifically on the selected targets. However, it is crucial to fully comprehend the action of the second generation of drugs and their mechanisms that involve the phototherapeutic process of PDT, so that the treatment is employed with maximum efficiency, without having negative effects like Firczuk *et al.*, Korbelik *et al.*, and Casas *et al.*, describe with the studies on resistance to PDT in cancer cells.[43–45]

In this way, comparing the results of the crystal violet test, Xin *et al.*[40] verified that conjugated drugs have a greater phototherapeutic effect than the free photosensitizer, reducing the population of cells in the clonogenic test. However, our results demonstrate that AlPcS4 in its free form has high efficiency, reducing the population of HEp-2 cells to less than 30% of survivors. However, both studies were performed using different cell lines, being therefore one of the reasons for the divergent results, since each lineage has its own metabolism. In addition, it can be seen that in the experiments of Xin *et al.*, PDT was performed using the wavelength of 635 nm, which lies far from the Q peak (675 nm) as demonstrated by the very Xin, can contribute to inefficiency of PDT using AlPcS4 in its free form.[40]

Moreover, Gijsens *et al.* and Castilho-Fernandes *et al.* used the mitochondrial activity assays to evaluate the novel drugs synthesized using AlPcS4. In both studies, the obtained results are similar to the one described by Xin *et al.*, because they demonstrate that conjugated or encapsulated drugs were more effective than the free form of the photosensitizer; however, in our study the efficacy of free drug compared to the control group is highly evident.[40–42]

Mitochondrial activity assay is performed with the reduction of the MTT salt, being absorbed by the cells and converted inside the mitochondria into formazan crystals.[46]

The oxidative damage generated from the interaction of excited molecular oxygen induces cells to become unviable, as singlet oxygen reacts with subcellular structures for its molecular stabilization, and in this way, it reacts with cell membrane, mitochondria, lysosomes and nucleus, causing deleterious damage at reaction sites compromising cell integrity.[21,47–49]

This oxidative process can be observed using the apoptosis assay, as the triggered stimulus for this type of cell death occurs from an internal damage in the cell. Consequently, the results evidenced by the viability and mitochondrial activity tests are confirmed by the data obtained with the apoptosis assay, as the control groups exhibited approximately 60% of living cells in the 24 and 48-h periods. However, the PDT groups demonstrated an expressive increase of apoptotic cells reaching over 50% of cells in both periods evidencing the death process from the oxidative damage of the treatment.

According to Xin *et al.*, PDT raises the process of apoptosis and necrosis. Results are similar to those obtained with the apoptosis assay, as the PDT can generate reactive species inside and outside the cells, depending only on the presence of photosensitizers and molecules such as oxygen, triggering a process of signaling cell death with the presence of markers such as Caspase 3, as described by Nonaka *et al.* [40,50]

Oxidative damage to DNA bases results in lesions caused by its reaction with ROS. These lesions may occur due to direct oxidation of nucleic acids, which may lead to breaks in one of the DNA strands (single strand break) or single breaks at positions approximately symmetrical in two DNA strands (double strand break). In addition, simple breaks can lead to double breaks during cell replication.[51]

Continuing the DNA damage study, according to Glei *et al.*,[52] the comet assay allows the analysis of evident damage to the genetic material of cells. The comet assay principle is that cell lysis exposes the genetic material to agarose gel, after which an electric potential difference is applied, thus causing the DNA to fragment. This drag can be measured by the OpenComet plug-in for the Image J software, which analyzes multiple parameters, as shown by Glei *et al.*[52] However, three measures are given to assess DNA damage, percentage of DNA in the tail, tail moment, and Olive Moment. In the present study, we used the percentage of DNA in the tail and Olive Moment. The percentage of DNA in the tail gives the tail DNA content as a percentage of comet DNA content, and the Olive Moment is a product of the tail DNA and the distance between the intensity-weighted centroids of the head and tail; thus, being an arbitrary unit.[52]

Analysis of the results obtained in the comet assay given in Tables 1 and 2 showed that in both the percentage of DNA in the comet tail and the Olive Moment genetic material cell integrity was not compromised, since the Control group expressed a median of 6.282% DNA in the comet tail in the observation period of 24 h in contrast to the PDT group with 88.12%. These data were confirmed when the Olive Moment at 24 h was analyzed. When the Control group was compared to the PDT group using the Olive Moment, it was statistically different. These data can suggest that the degree of toxicity generated instantly after PDT has a sharp relevance to the damage to the genetic material of cells exposed to the PDT treatment; the ROS reacts not only with active organelles, such as mitochondria and reticules, but also affects the cell as a whole, damaging the nuclear membrane and even its DNA.[3,8,53]

After 48 h, the Control group also presented an increase in relation to the 24-h period. The cell data median was even 22.23% smaller than that of the PDT group, and the percentage DNA median of the comet tail was 49.66%. Such analysis was again confirmed by the Olive Moment when both groups were compared. It is worth noting that the degree of damage to the genetic material in the PDT group decreased, but it is necessary to correlate the treatment time with the cell cycle in question. Cells tested for 48 h were no longer the same as the cells that suffered direct damage under 24 h of analysis, since the eukaryotic cell cycle lasts approximately 24 h.[54]

The last test used to confirm the interaction between PDT and DNA damage in cancer cells, the micronucleus assay, allows analyzing genotoxicity and DNA damage caused during the cell interphase. It is an important test as an alternative to the karyotype in the identification of possible loss of chromosomal material. Moreover, the micronucleus counting method is easy to apply, since the cell is parked during the interphase layer and the DAPI dye easily binds to the genetic material. The images are acquired by fluorescence microscopy and the micronuclei formed are counted. [26,55–57]

Comparison of Control and PDT and EMS and PDT data at 24 h revealed differences in micronucleus frequency at 48 h; the difference remained statistically significant. Comparison of the Control group, without any treatment, and the EMS group, the positive Control for micronucleus, revealed a difference in the two periods analyzed.

A significant increase in micronuclei frequency was also noticed in the Control and EMS groups when the 24 h and 48 h periods were compared, in contrast to the PDT group, which did not present any difference between the periods.

Therefore, the cells can choose one of two strategies – first, to repair the damages caused to its DNA or even tolerate such damages, or, second, to remove the cell population by killing the cells. Besides causing damage to diverse cell structures and mainly to the DNA of cancer cells, the production of ROS by PDT provides a cell cycle malfunction scenario, as evidenced by the increase in the number of micronuclei formed (tentative repair and damage tolerance scenario) and also cell death, as evidenced by the decrease in the cell population in the violet crystal test (cell death scenario).[12]

Although apoptosis and the MN assays showed a certain visual similarity, their overall biochemical spectra differed, since apoptosis is a typical form of cell death characterized by cell shrinkage, dramatic rearrangement of the cell nucleus, organized cleavage into 200–300 and 30–50 kb pieces, and final fragmentation of the cell into

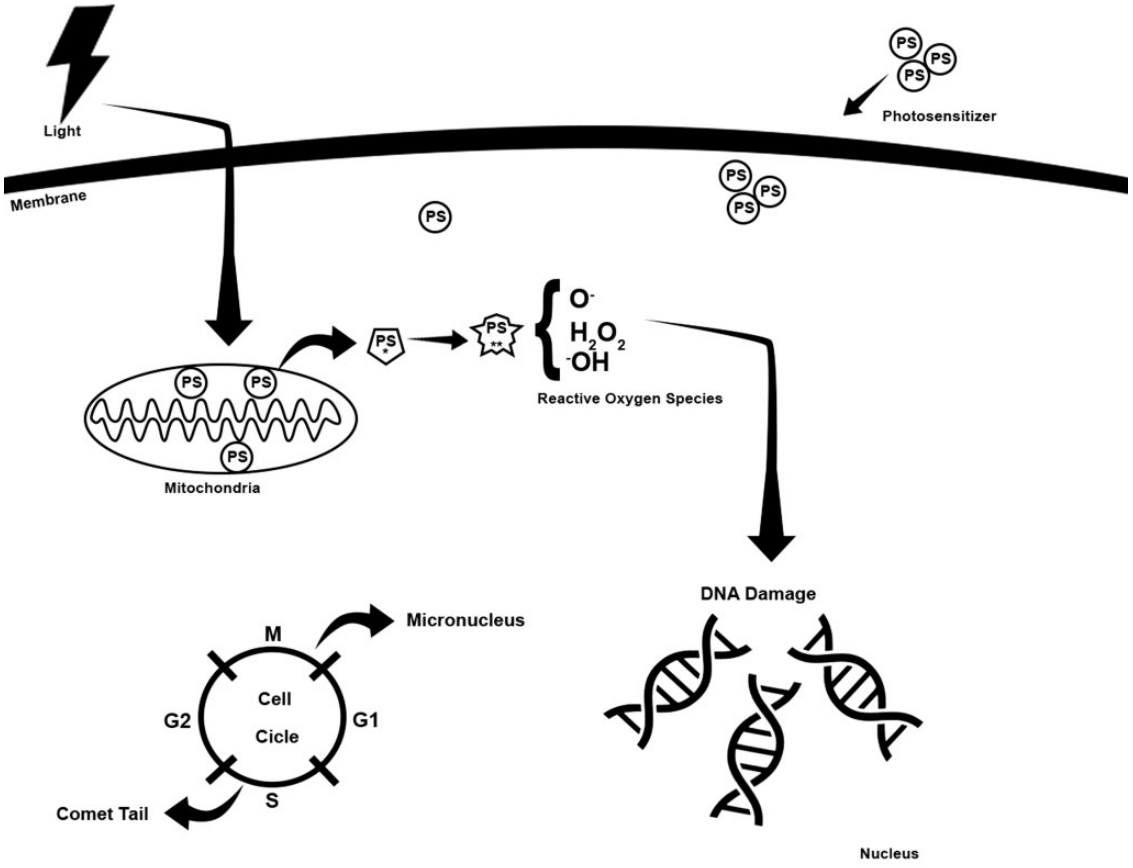

Figure 6. Illustration about the action mechanism of photodynamic therapy in DNA damage proposed.

membrane-cleated vesicles. However, the MN did not present these characteristics, since the cell DNA cleavage occurred in a random and disproportionate manner, and there was no general cell structural change.[19]

It is known that DNA repair is closely intertwined with the regulation of the cell cycle, transcription, and replication and that in part these mechanisms use common factors. Therefore, if lesions are not removed, they can lead to death or result in the incorporation of mutations into the genome and their transmission to future generations.[51]

Furthermore, in the study of cells it is known that physiological mechanisms such as cell proliferation and death are needed for the maintenance of the cell population. However, it can be also pointed out that cancer cells present fundamental changes in the genetic control of cell division, resulting in unrestricted cell proliferation and loss of genetic quality between stem cells and daughters.[58] Moreover, inactivation of tumor suppressor genes such as pRb and p53 results in the dysfunction of proteins that normally inhibit cell cycle progression. As also noted in the literature, deregulation of the cell cycle associated with cancer occurs by mutation of important proteins at different levels of the cell cycle.[12,58]

The effect of PDT-produced ROS and the resulting damage to several subcellular components has been correlated with cell cycle phases. Analysis of the comet assay results suggests that ROS causes damage to the DNA of cancer cells specifically in the DNA synthesis phase of the cell cycle (S), when the DNA of the cell is duplicated, being thus more exposed to possible damages. Therefore, it may be suggested that the comet assay evidences the damage caused by ROS, which is observed in the comet tail drag. This scenario demonstrates the fact that cancer cells lack additional controls or checkpoints and correction of DNA damage, causing damage to the genetic material of cells surviving the PDT treatment.[12,51,52,58–60]

In response to the DNA damage, the checkpoints normally disrupt the cell cycle to provide time for DNA repair. However, as the target of the damage caused by ROS is a cancer cell, the checkpoints are not so efficient in the correction of the damages caused by PDT, because these points are positioned before the cell enters the S phase (G1 checkpoint-S) or after DNA replication (G2 checkpoint-M). Therefore, it is possible to observe the formation of micronuclei as a result of the damage caused to the cancer cell DNA, which is evidenced by the micronucleus assay and thus demonstrating the genotoxicity of the treatment to cancer cells.[19,53,58,60] The mechanism proposed for the action of PDT in DNA damage is illustrated in Figure 6.

Finally, PDT is a cytotoxic treatment, as demonstrated by the violet crystal assay, and that it can also be considered genotoxic, as evidenced by the comet and micronucleus

assays. Thus, photodynamic therapy presents an interesting potential for the treatment of cancer cells, resulting in damage to several cell compartments, one of which is the DNA of the cancer cells.

Authors' contributions: All authors participated in the design, studies interpretation and data analysis, and in the manuscript review; CDGOM, BHG, ICSC, JCP and RCR conducted the experiments, NSS and CPS supplied all reagents for the experiments, and all authors participated in the manuscript writing.

DECLARATION OF CONFLICTING INTERESTS

The author(s) declared no potential conflicts of interest with respect to the research, authorship, and/or publication of this article.

FUNDING

The authors acknowledge the support from FAPESP (Fundação de Amparo a Pesquisa do Estado de São Paulo – São Paulo Research Foundation, Contract grant number 2013/20054–8) and CNPq (Conselho Nacional de Desenvolvimento Científico e Tecnológico – National Council for Scientific and Technological Development (PIBIC – Programa Institucional de Bolsas de Iniciação Cientifica – Institutional Program for Scientific Initiation Grants) Grant- Process: 115582/2016–9 Modality– Category: Scientific Initiation – (IC) – Validity Period: Jan. 08, 2016 to Jul. 31, 2017). And Part of this study was also financed by the Coordination for the Improvement of Higher Education Personnel (CAPES) – Finance Code 001.

ORCID iD

Cristina Pacheco Soares http://orcid.org/0000-0002-0572-074X

REFERENCES

1. Nunes SMT, Sguilla FS, Tedesco AC. Photophysical studies of zinc phthalocyanine and chloroaluminum phthalocyanine incorporated into liposomes in the presence of additives. *Braz J Med Biol Res* 2004;**37**:273–84
2. Chan CMH, Lo P-C, Yeung S-L, Ng DKP, Fong W-P. Photodynamic activity of a glucoconjugated silicon(IV) phthalocyanine on human colon adenocarcinoma. *Cancer Biol Ther* 2010;**10**:126–34
3. Lin S, Zhang L, Lei K, Zhang A, Liu P, Liu J. Development of a multifunctional luciferase reporters system for assessing endoplasmic reticulum-targeting photosensitive compounds. *Cell Stress Chaperones* 2014;**19**:927–37
4. Galvão LEG, H de S G, Caldas JC, Cavalcante CM. Daylight photodynamic therapy: pharmacoeconomics of methyl aminolevulinate cream use for facial actinic keratoses. *Surg Cosmet Dermatology* 2016;**8**:246–9
5. Vittar NBR, Awruch J, Azizuddin K, Rivarola V. Caspase-independent apoptosis, in human MCF-7c3 breast cancer cells, following photodynamic therapy, with a novel water-soluble phthalocyanine. *Int J Biochem Cell Biol* 2010;**42**:1123–31
6. Castano AP, Demidova TN, Hamblin MR. Mechanisms in photodynamic therapy: part two – cellular signaling, cell metabolism and modes of cell death. *Photodiagnosis Photodyn Ther* 2005;**2**:1–23
7. Vasconcelos RC. *Efeitos da terapia fotodinâmica com alumínio – cloro ftalocianina sobre a peroxidação lipídica e produtos antioxidantes em tecidos inamados animais*. Rio Grande do Norte-Brazil: Universidade Federal Do Rio Grande Do Norte, 2016
8. Pazos M, de C, Ricci R, Simioni AR, Lopes CC, Tedesco AC, Nader HB. Putative role of heparan sulfate proteoglycan expression and shedding on the proliferation and survival of cells after photodynamic therapy. *Int J Biochem Cell Biol* 2007;**39**:1130–41
9. Tedesco AC, Sousa G, Zângaro RA, Silva NS, Pacheco MTT, Pacheco-Soares C, Ferreira SDRM. Analysis of mitochondria, endoplasmic reticulum and actin filaments after PDT with AlPcS(4). *Lasers Med Sci* 2004;**18**:207–12
10. Torezan L, Niwa ABM, Festa Neto C. Terapia fotodinâmica em dermatologia: princípios básicos e aplicações. *An Bras Dermatol* 2009;**84**:445–59
11. Fonseca MDO. *Inuência do Cortisol no Desenvolvimento de Células Tumorais Inuência do Cortisol no Desenvolvimento de Células Tumorais*. São Jose dos Campos-São Paulo-Brazil: Universidade Do Vale Do Paraiba, 2014
12. Roos WP, Kaina B. DNA damage-induced cell death by apoptosis. *Trends Mol Med* 2006;**12**:440–50
13. Lacerda MF Lopes Santos, Alfenas CF, Campos CN. Terapia fotodinâmica associada ao tratamento endodôntico convencional. *Rev da Fac Odontol* 2014;**19**:115–20
14. Silva AP. *Avaliação histopatológica do tratamento do carcinoma espinocelular cutâneo em camundongos usando terapia fotodinâmica mediada por azul de metileno*. São Paulo-São Paulo-Brazil: Universidade De São Paulo, 2014
15. Dutra DAM. *Avaliação do fotossensibilizador azul de metileno em diferentes formulações para uso em terapia fotodinâmica*. Santa Maria-Rio Grande do Sul-Brazil: Universidade Federal De Santa Maria, 2013.
16. Amaral RR, Nunes E, Soares JA, Silveira FF. Terapia fotodinâmica na endodontia - revisão de literatura. *RFO UPF* 2010;**15**:207–11
17. Amaral GP. *Estudo das propriedades antioxidantes de diferentes ftalocianinas*. Santa Maria- Rio Grande do Sul-Brazil: Universidade Federal De Santa Maria, 2013
18. Silva CV. *Sistema lipossomal de ftalocianina de cloro-alumínio, contendo ácido fólico, aplicada à Terapia Fotodinâmica*. São Paulo-São Paulo-Brazil: Universidade de São Paulo, 2013
19. Earnshaw WC. Nuclear changes in apoptosis. *Curr Opin Cell Biol* 1995;**7**:337–43
20. Machado AHA, Pacheco Soares C, da Silva NS, Moraes KCM. Cellular and molecular studies of the initial process of the photodynamic therapy in HEp-2 cells using LED light source and two different photosensitizers. *Cell Biol Int* 2009;**33**:785–95.
21. Fontana LC, Pinto JG, Pereira AHC, Soares CP, Raniero LJ, Ferreira-Strixino J. Photodithazine photodynamic effect on viability of 9L/lacZ gliosarcoma cell line. *Lasers Med Sci* 2017;**32**:1245–52
22. Pacheco-Soares C, Maftou-Costa M, Da Cunha Menezes Costa CG, De Siqueira Silva AC, Moraes KCM. Evaluation of photodynamic therapy in adhesion protein expression. *Oncol Lett* 2014;**8**:714–8
23. Feoktistova M, Geserick P, Leverkus M. Crystal violet assay for determining viability of cultured cells. *Cold Spring Harb Protoc* 2016;**2016**: pdb.prot087379
24. Charalambous C, Pitta CA, Constantinou AI. Equol enhances tamoxifen's anti-tumor activity by induction of caspase-mediated apoptosis in MCF-7 breast cancer cells. *BMC Cancer* 2013;**13**:238
25. Gyori BM, Venkatachalam G, Thiagarajan PS, Hsu D, Clement M-V. OpenComet: an automated tool for comet assay image analysis. *Redox Biol*. 2014;**2**:457–65
26. Carvalho ICS, Dutra TP, De Andrade DP, Balducci I, Pacheco-Soares C, Rocha RF. D. High doses of alcohol during pregnancy cause DNA damages in osteoblasts of newborns rats. *Birth Defects Res Part A Clin Mol Teratol* 2016;**106**:122–32
27. Singh NP, McCoy MT, Tice RR, Schneider EL. A simple technique for quantitation of low levels of DNA damage in individual cells. *Exp Cell Res* 1988;**175**:184–91
28. Da Silva J, De Freitas TRO, Marinho JR, Speit G, Erdtmann B. An alkaline single-cell gel electrophoresis (comet) assay for environmental biomonitoring with native rodents. *Genet Mol Biol* 2000;**23**:241–5
29. Tian Y, Shen L, Gao Y, Yamauchi T, Shen X, Ma N. Comparison of 4′, 6′-diamidino-2-phenylindole and Giemsa stainings in preimplantation mouse embryos micronucleus assay including a triple dose study. *Ind Health* 2007;**45**:343–7

30. Kirsch-Volders M, Sofuni T, Aardema M, Albertini S, Eastmond D, Fenech M, Ishidate M, Kirchner S, Lorge E, Morita T, Norppa H, Surrallés J, Vanhauwaert A, Wakata A. Report from the in vitro micronucleus assay working group. *Mutat Res* 2003;**540**:153–63
31. Lasne C, Gu ZW, Venegas W, Chouroulinkov I. The in vitro micronucleus assay for detection of cytogenetic effects induced by mutagen carcinogens – comparison with the in vitro sister-chromatid exchange assay. *Mutat Res* 1984;**130**:273–82
32. Fenech M. Cytokinesis-block micronucleus cytome assay. *Nat Protoc* 2007;**2**:1084–104
33. Nersesyan A, Fenech M, Bolognesi C, Mišík M, Setayesh T, Wultsch G, Bonassi S, Thomas P, Knasmüller S. Use of the lymphocyte cytokinesis-block micronucleus assay in occupational biomonitoring of genome damage caused by in vivo exposure to chemical genotoxins: past, present and future. *Mutat Res Mutat Res* 2016;**770**:1–11
34. Titenko-Holland N, Windham G, Kolachana P, Reinisch F, Parvatham S, Osorio A, Smith M. Genotoxicity of malathion in human lymphocytes assessed using the micronucleus assay in vitro and in vivo: a study of malathion-exposed workers. *Mutat Res Toxicol Environ Mutagen* 1997;**388**:85–95
35. Labanauskienė J, Šatkauskas S, Kirvelienė V, Venslauskas M, Atkočius V, Didžiapetrienė J. Enhancement of photodynamic tumor therapy effectiveness by electroporation in vitro. *Medicina* 2009;**45**:372
36. Wu X, Zhang F, Chen R, Zheng W, Yang X. Recent advances in imaging-guided interventions for prostate cancers. *Cancer Lett* 2014;**349**:114–9
37. McCAUGHAN JS. Photodynamic therapy of endobronchial and esophageal tumors: an overview. *J Clin Laser Med Surg* 1996;**14**:223–33
38. Zenoni SA, Arnoletti JP, de la Fuente SG. Recent developments in surgery. *JAMA Surg* 2013;**148**:1154
39. Silva ACDS. *Caracterização de células resistentes a terapia fotodinâmica*. São Jose dos Campos- São Paulo-Brazil: Universidade Do Vale Do Paraíba, 2014
40. Xin J, Wang S, Wang B, Wang J, Wang J, Zhang L, Xin B, Shen L, Zhang Z, Yao C. AlPcS4-PDT for gastric cancer therapy using gold nanorod, cationic liposome, and Pluronic® F127 nanomicellar drug carriers. *Int J Nanomedicine* 2018;**13**:2017–36
41. Gijsens A, Derycke A, Missiaen L, De Vos D, Huwyler J, Eberle A, De Witte P. Targeting of the photocytotoxic compound A1PcS4 to Hela cells by transferrin conjugated PEG-liposomes. *Int J Cancer* 2002;**101**:78–85
42. Castilho-Fernandes A, Lopes TG, Primo FL, Pinto MR, Tedesco AC. Photodynamic process induced by chloro-aluminum phthalocyanine nanoemulsion in glioblastoma. *Photodiagnosis Photodyn Ther* 2017;**1**:221–8
43. Firczuk M, Gabrysiak M, Barankiewicz J, Domagala A, Nowis D, Kujawa M, Jankowska-Steifer E, Wachowska M, Glodkowska-Mrowka E, Korsak B, Winiarska M, Golab J. GRP78-targeting subtilase cytotoxin sensitizes cancer cells to photodynamic therapy. *Cell Death Dis* 2013;**4**:e741–e741
44. Korbelik M, Sun J, Cecic I. Photodynamic therapy-induced cell surface expression and release of heat shock proteins: relevance for tumor response. *Cancer Res* 2005;**65**:1018–26
45. Casas A, Di Venosa G, Hasan T. Al Batlle. Mechanisms of resistance to photodynamic therapy. *Curr Med Chem* 2011;**18**:2486–515
46. Mosmann T. Rapid colorimetric assay for cellular growth and survival: application to proliferation and cytotoxicity assays. *J Immunol Methods* 1983;**65**:55–63
47. Ramos LDP. *Atividade antimicrobiana e citotoxicidade dos extratos glicólicos de Pfafa paniculata K. E Juglans regia L*. São Jose dos Campos-São Paulo-Brazil: Universidade Estadual Paulista, 2016
48. Mroz P, Yaroslavsky A, Kharkwal GB, Hamblin MR. Cell death pathways in photodynamic therapy of cancer. *Cancers* 2011;**3**:2516–39
49. Allison RR. Photodynamic therapy: oncologic horizons. *Future Oncol* 2014;**10**:123–4
50. Nonaka T, Nanashima A, Nonaka M, Uehara M, Isomoto H, Asahina I, Nagayasu T. Analysis of apoptotic effects induced by photodynamic therapy in a human biliary cancer cell line. *Anticancer Res* 2010;**30**:2113–8
51. Berra CM, Menck CFM. Estresse oxidativo, lesões no genoma, processos de sinalização e controle do ciclo celular. *Quím Nova* 2006;**29**:1340–4
52. Glei M, Schneider T, Schlörmann W. Comet assay: an essential tool in toxicological research. *Arch Toxicol* 2016;**90**:2315–36
53. Issa M, Manela-Azulay M. Photodynamic therapy: a review of the literature and image documentation. *An Bras Dermatol* 2010;**85**:501–11
54. Cooper MG. *The cell: a molecular approach*. *The eukaryotic cell cycle*. Chapter 14, Second Edition, 2000
55. Flores M, Yamaguchi MU. Teste do micronúcleo: uma triagem para avaliação genotóxica. *Rev Saúde e Pesqui* 2008;**1**:337–40
56. Garriott ML, Barry Phelps J, Hoffman WP. A protocol for the *in vitro* micronucleus test: I. Contributions to the development of a protocol suitable for regulatory submissions from an examination of 16 chemicals with different mechanisms of action and different levels of activity. *Mutat Res* 2002;**517**:123–34
57. Kirsch-Volders M, Decordier I, Elhajouji A, Plas G, Aardema MJ, Fenech M. In vitro genotoxicity testing using the micronucleus assay in cell lines, human lymphocytes and 3D human skin models. *Mutagenesis* 2011;**26**:177–84
58. Vermeulen K, Van Bockstaele DR, Berneman ZN, Vermeulen K, Van Bockstaele DR, Berneman ZN. The cell cycle: a review of regulation, deregulation and therapeutic targets in cancer. *Cell Prolif* 2003;**36**:131–49
59. Lee W-Y, Chen Y-C, Shih C-M, Lin C-M, Cheng C-H, Chen K-C, Lin C-W. The induction of heme oxygenase-1 suppresses heat shock protein 90 and the proliferation of human breast cancer cells through its byproduct carbon misionoxide. *Toxicol Appl Pharmacol* 2014;**274**:55–62
60. Lang F, Ritter M, Gamper N, Huber SM, Fillon S, Tanneur V, Lepple-Wienhues A, Szabo I, Gulbins E, Cellular P. Biochemistry cell volume in the regulation of cell proliferation and apoptotic cell death. *Cell Physiol Biochem* 2000;**10**:417–28

(Received September 10, 2018, Accepted January 7, 2019)